

Cell Reports, Volume 37

## Supplemental information

### **Functional drug susceptibility testing using single-cell mass predicts treatment outcome in patient-derived cancer neurosphere models**

**Max A. Stockslager, Seth Malinowski, Mehdi Touat, Jennifer C. Yoon, Jack Geduldig, Mahnoor Mirza, Annette S. Kim, Patrick Y. Wen, Kin-Hoe Chow, Keith L. Ligon, and Scott R. Manalis**

**Table S1. Identification and origin of the 69 patient-derived neurosphere models.** Abbreviations: CPDM (Center for Patient Derived Models, Dana Farber Cancer Institute); CCLF (Cancer Cell Line Factory, Broad Institute); NA (data not available). Related to STAR Methods.

	<b>Record ID</b>	<b>Patient ID</b>	<b>CPDM ID</b>	<b>BT ID</b>	<b>CCLF ID2</b>	<b>Origin</b>	<b>Sex</b>
1	BT112	10043_0034	CPDM_1272X	BT112	BT112	Ligon tissue bank	Male
2	BT131	10043_0051	CPDM_1275X	BT131	BT131	Ligon tissue bank	Male
3	BT139	10043_0058	CPDM_1276X	BT139	BT139	Ligon tissue bank	Male
4	BT145	10043_0063	CPDM_1279X	BT145	BT145	Ligon tissue bank	Male
5	BT147	10043_0065	CPDM_1280X	BT147	BT147	Ligon tissue bank	Male
6	BT159	10043_0074	CPDM_1282X	BT159	BT159	Ligon tissue bank	Female
7	BT164	10043_0079	CPDM_0885X	BT164	CCLF_KL1429	Ligon tissue bank	Female
8	BT168	10043_0021	CPDM_1283X	BT168	BT168	Ligon tissue bank	Female
9	BT172	10043_0086	CPDM_1284X	BT172	BT172	Ligon tissue bank	Female
10	BT179	10043_0092	CPDM_1285X	BT179	BT179	Ligon tissue bank	Female
11	BT181	10043_0094	CPDM_1286X	BT181	BT181	Ligon tissue bank	Female
12	BT188	10043_0100	CPDM_1459X	BT188	BT188	Ligon tissue bank	Female
13	BT189	10043_0101	CPDM_0796X	BT189	NA	Ligon tissue bank	Male
14	BT216	10043_0124	CPDM_1289X	BT216	BT216	Ligon tissue bank	Female
15	BT224	10043_0128	CPDM_1458X	BT224	BT224	Ligon tissue bank	Male
16	BT228	10043_0131	CPDM_0887X	BT228	BT228	Ligon tissue bank	Female
17	BT231	10043_0134	NA	BT231	NA	Ligon tissue bank	Male
18	BT232	10043_0135	CPDM_1270X	BT232	BT232	Ligon tissue bank	Male
19	BT239	10043_0139	CPDM_1290X	BT239	BT239	Ligon tissue bank	Male
20	BT245	10043_0143	CPDM_0797X	BT245	BT245	Ligon tissue bank	Male
21	BT248	10043_0145	CPDM_1292X	BT248	BT248	Ligon tissue bank	Female
22	BT271	10043_0163	CPDM_1592X	BT271	NA	Ligon tissue bank	Male
23	BT286	10-417-83	CPDM_0812X	BT286	BT286	Ligon tissue bank	Male
24	BT295	10043_0177	CPDM_1294X	BT295	BT295	Ligon tissue bank	Female
25	BT320	10043_0190	CPDM_1295X	BT320	BT320	Ligon tissue bank	Male
26	BT328	10-417-65	CPDM_1297X	BT328	BT328	Ligon tissue bank	Male
27	BT329	10-417-469	CPDM_1478X	BT329	CCLF_KL1252	Ligon tissue bank	Female
28	BT330	10043_0163	CPDM_1298X	BT330	BT330	Ligon tissue bank	Male
29	BT333	10043_0194	CPDM_0886X	BT333	BT333	Ligon tissue bank	Female
30	BT340	10-417-31	CPDM_1299X	BT340	CCLF_KL1433	Ligon tissue bank	Male
31	BT359	10-417-107	CPDM_1300X	BT359	BT359	Ligon tissue bank	Male
32	BT360	10-417-109	CPDM_1301X	BT360	BT360	Ligon tissue bank	Male
33	BT394	10-417-456	CPDM_1304X	BT394	CCLF_KL1250	Ligon tissue bank	Male
34	BT416	10-417-574	CPDM_0809X	BT416	BT416	Ligon tissue bank	Female
35	BT422	10-417-5032	CPDM_0888X	BT422	CCLF_KL1254	Ligon tissue bank	Female

(continued on next page)

	<b>Record ID</b>	<b>Patient ID</b>	<b>CPDM ID</b>	<b>BT ID</b>	<b>CCLF ID2</b>	<b>Origin</b>	<b>Sex</b>
36	BT428	10-417-605	CPDM_1313X	BT428	BT428	Ligon tissue bank	Male
37	BT440	10043_0210	CPDM_1316X	BT440	BT440	Ligon tissue bank	Female
38	BT444	10-417-755	CPDM_1317X	BT444	BT444	Ligon tissue bank	Male
39	BT458	10-417-863	CPDM_1320X	BT458	BT458	Ligon tissue bank	Male
40	BT482	10043_0215	CPDM_0884X	BT482	BT482	Ligon tissue bank	Male
41	BT504	10-417-1200	CPDM_1327X	BT504	BT504	Ligon tissue bank	Female
42	BT509	10-417-1273	CPDM_1328X	BT509	BT509	Ligon tissue bank	Male
43	BT519	10-417-1362	CPDM_1331X	BT519	CCLF_KL1256	Ligon tissue bank	Female
44	BT530	10-417-1436	CPDM_1334X	BT530	BT530	Ligon tissue bank	Female
45	BT559	10-417-1743	CPDM_1336X	BT559	CCLF_KL1431	Ligon tissue bank	Female
46	BT574	10-417-2100	CPDM_1338X	BT574	CCLF_KL1249	Ligon tissue bank	Female
47	BT632	10-417-2633	CPDM_0098X	BT632	Ag1052	Ligon tissue bank/CCLF	Male
48	BT633	10-417-2030	CPDM_1342X	BT633	CCLF_KL1248	Ligon tissue bank	Female
49	BT639	10-417-2831	CPDM_1343X	BT639	BT639	Ligon tissue bank	Female
50	BT681	10-417-2105	CPDM_1346X	BT681	BT681	Ligon tissue bank/CCLF	Male
51	BT699	10-417-2858	CPDM_1347X	BT699	CCLF_KL1247	Ligon tissue bank	Female
52	BT701	10-417-3189	CPDM_1348X	BT701	BT701	Ligon tissue bank	Female
53	BT715	10-417-3566	CPDM_1351X	BT715	BT715	Ligon tissue bank	Male
54	BT774	10-417-4326	CPDM_1353X	BT774	NA	Ligon tissue bank/CCLF	Male
55	BT779	10-417-4403	CPDM_1354X	BT779	BT779	Ligon tissue bank/CCLF	Male
56	BT790	10-417-4506	CPDM_1355X	BT790	BT790	Ligon tissue bank	Female
57	BT820	10-417-4642	CPDM_1357X	BT820	BT820	Ligon tissue bank	Female
58	BT924	10-417-5394	CPDM_0094X	BT924	Ag1011	Ligon tissue bank/CCLF	Male
59	BT954	10-417-5075	CPDM_0093X	BT954	Ag1033	CCLF	Male
60	BT1153	10-417-6613	CPDM_0102X	BT1153	CCLF_KL1060	Ligon tissue bank	Male
61	BT1160	10-417-6654	CPDM_0103X	BT1160	CCLF_KL1066	Ligon tissue bank/CCLF	Female
62	BT1707	10043_0261	CPDM_1587X	BT1707	NA	Ligon tissue bank	Male
63	BT1718	10-417-9107	NA	BT1718	NA	Ligon tissue bank	Female
64	BT1719	10-417-9137	NA	BT1719	NA	Ligon tissue bank	Female
65	CPDM_0004X	10-417-6950	CPDM_0004X	NA	NA	CPDM	Male
66	CPDM_0051X	10-417-5188	CPDM_0051X	NA	NA	CPDM	Female
67	CPDM_0095X	10-417-5861	CPDM_0095X	BT1018	Ag1032	Ligon tissue bank/CCLF	Female
68	CPDM_0097X	10-417-5396	CPDM_0097X	BT923	NA	Ligon tissue bank/CCLF	Female
69	N16-1162	NA	NA	NA	NA	Paris Brain Institute	Female

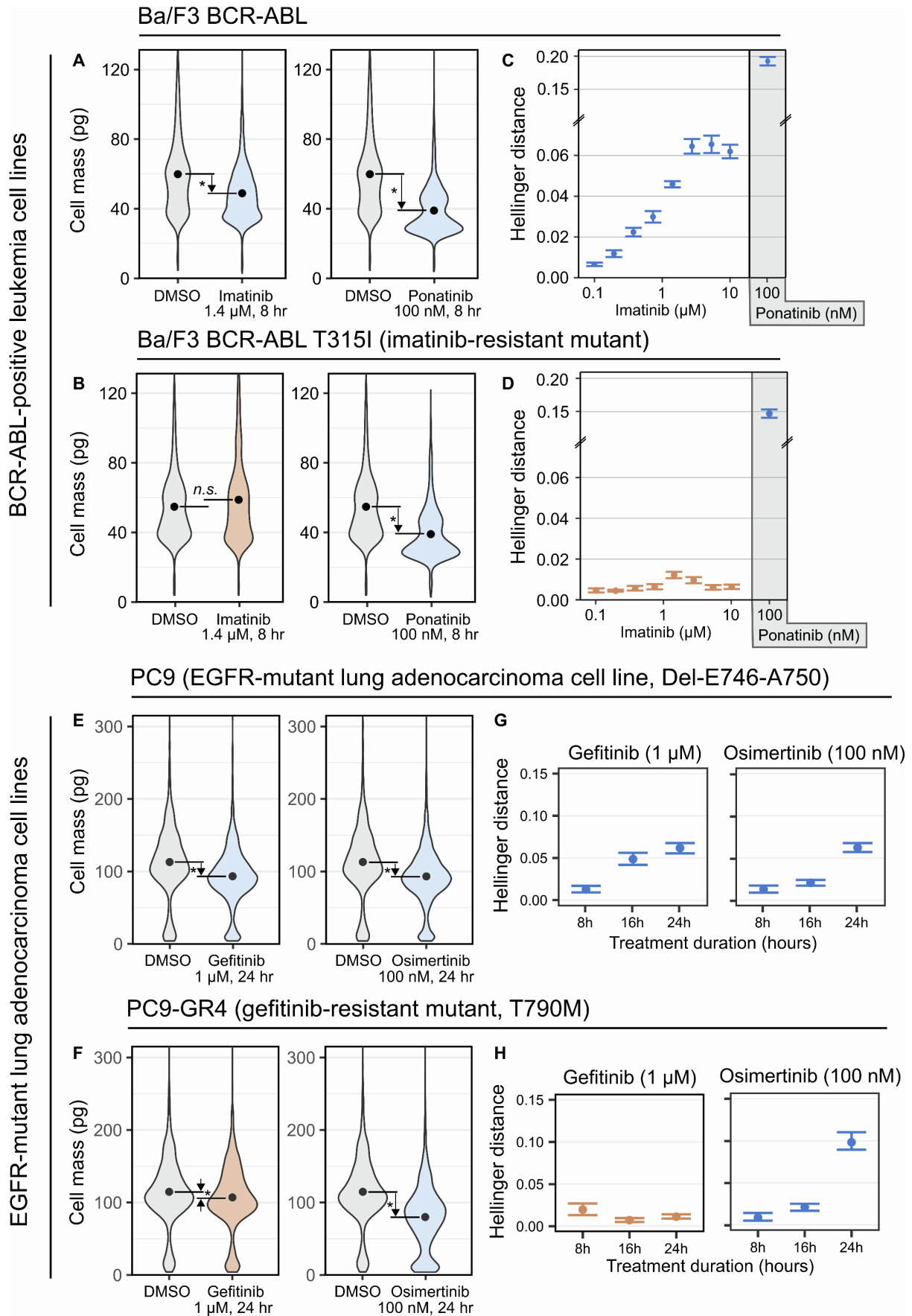
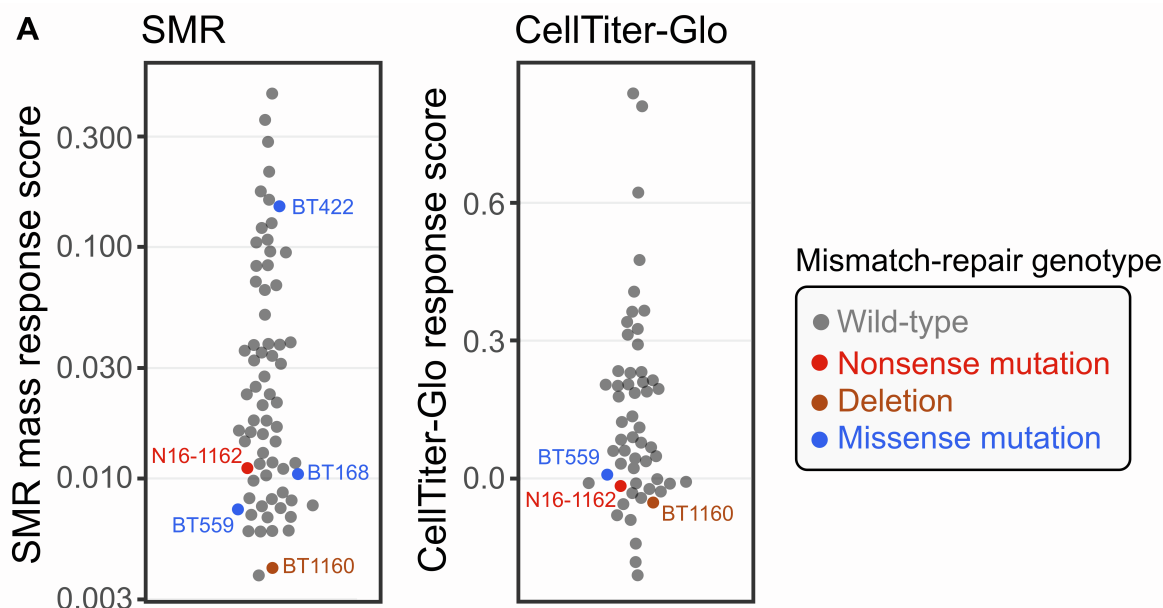


**Figure S1. The SMR mass assay recapitulates expected patterns of drug sensitivity and resistance in BCR-ABL-positive leukemia and EGFR-mutant lung cancer cell lines.** (A) Imatinib and ponatinib drug responses observed in Ba/F3 BCR-ABL. For Ba/F3 BCR-ABL, there is a significant reduction in mean cell mass after 8 hours exposure to 1.4  $\mu$ M imatinib (one-sided Wilcoxon rank-sum  $p < 10^{-3}$ ) and to 100 nM ponatinib (one-sided Wilcoxon rank-sum  $p < 10^{-3}$ ). Minimum 2200 cells measured per condition. (B) Imatinib and ponatinib drug responses observed in Ba/F3 BCR-ABL T315I. As expected, for Ba/F3 BCR-ABL T315I, there is only a significant reduction in mean mass after 8 hours exposure to 100 nM ponatinib (one-sided Wilcoxon rank-sum  $p < 10^{-3}$ ), but not to 1.4  $\mu$ M imatinib (one-sided Wilcoxon rank-sum  $p > 0.99$ ). Minimum 2200 cells measured per condition. (C) Ba/F3 BCR-ABL imatinib dose-response curve measured using the SMR mass assay, given as Hellinger distance  $\pm$  bootstrap standard error. (D) Ba/F3 BCR-ABL T315I imatinib dose-response curve measured using the SMR mass assay, given as Hellinger distance  $\pm$  bootstrap standard error. (E) Gefitinib and osimertinib drug responses observed in PC9, an EGFR-mutant (Del-E746-A750) lung adenocarcinoma cell line expected to be sensitive to both EGFR inhibitors. For PC9, there is a large reduction in mean cell mass in response to 24 hours exposure to either 1  $\mu$ M gefitinib (16% reduction, one-sided Wilcoxon rank-sum  $p < 10^{-3}$ ) or to 100 nM osimertinib (16% reduction; one-sided Wilcoxon rank-sum  $p < 10^{-3}$ ). Minimum 3000 cells measured per condition. (F) Gefitinib and osimertinib drug responses observed in PC9-GR4, expected to be resistant to gefitinib but not to the second-generation EGFR inhibitor osimertinib. For PC9-GR4, there is only a small reduction in cell mass in response to 24 hours exposure to 1  $\mu$ M gefitinib (6% reduction, one-sided Wilcoxon rank-sum  $p < 10^{-3}$ ), but a larger reduction in response to 100 nM osimertinib (34% reduction; one-sided Wilcoxon rank-sum  $p < 10^{-3}$ ). Minimum 3000 cells measured per condition. (G) Time response for the PC9 cell line after exposure to EGFR inhibitors, given as Hellinger distance  $\pm$  bootstrap standard error. (H) Time response for the PC9-GR4 cell lines after exposure to EGFR inhibitors, given as Hellinger distance  $\pm$  bootstrap standard error. Related to “Validation of the SMR mass assay using conventional cancer cell lines” in STAR Methods.





**B** List of models with mismatch-repair (MMR) alterations

Model ID	MMR gene	Variant	Variant type	MGMT status
BT168	MSH2	T905I	Missense	Methylated (deficient)
BT422	PMS2	R20Q	Missense	Methylated (deficient)
BT559	MSH6	A457V, P107L	Missense	Methylated (deficient)
BT1160	MSH2	Homozygous deletion	Loss of function	Unmethylated (proficient)
N16-1162	MSH2	Q324*	Nonsense	Methylated (deficient)

**Figure S3. TMZ responsiveness in patient-derived models with mismatch-repair alterations.** Even in MGMT-methylated tumors, mismatch-repair deficiency (e.g., via an inactivating mutation) can also lead to TMZ resistance, as exposed cells can continue to cycle while accumulating a high mutational burden induced by the drug. **(A)** Consistently, the two models in our cohort with MMR-inactivating deletions or nonsense mutations (BT1160 and N16-1162) showed low functional TMZ responsiveness by both the SMR and CellTiter-Glo functional assays, despite N16-1162 having methylated MGMT and sequelae of MMR-deficiency (i.e., high tumor mutational burden). Three models harbored missense variants of unknown significance, of which two out of three (BT559 and BT168) showed functional TMZ resistance, while one (BT422) was highly responsive to TMZ. **(B)** Summary of MMR variants and MGMT status. Related to Fig. 4.

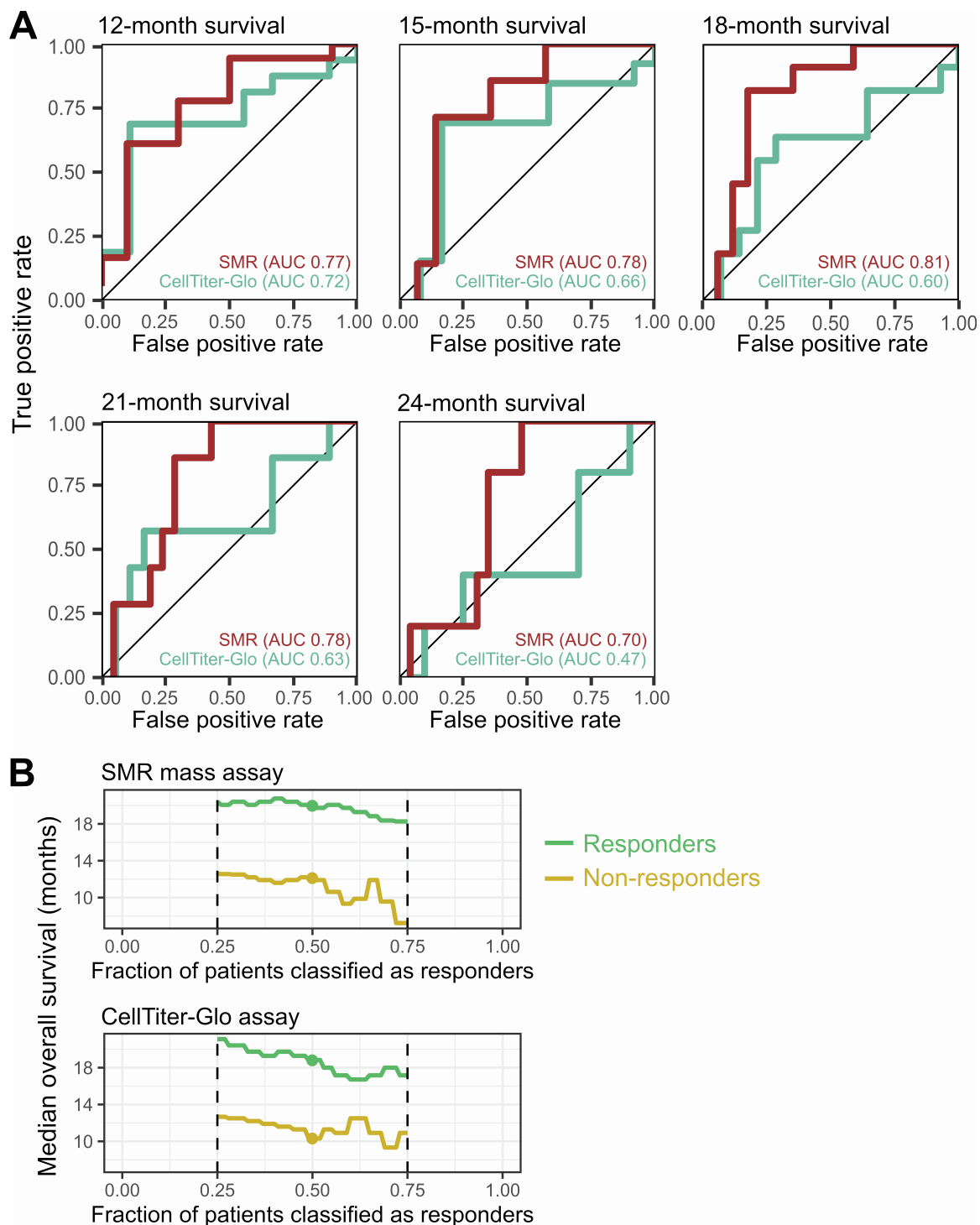


**Figure S4. Evaluating robustness of the results related to predicting overall survival duration. (A)** Predicting binary survival outcomes using functional biomarkers. Receiver operator characteristic for predicting 12-, 15-, 18-, 21- and 24-month survival using the SMR mass assay and CellTiter-Glo assay. Predictive power (here, quantified as the ROC AUC statistic) is similar regardless of the binary survival outcome used to set the decision threshold for classifying patients as responders versus non-responders. **(B)** Predictive power depends only weakly on the fraction of patients classified as responders. We chose to classify the top 50% of most-responsive patients as “responders” for each functional assay, because approximately half of GBM patients respond to TMZ. Changing this number (here, shown for the range of 25% to 75% of patients classified as responders) only weakly affects the predictive power of the functional assays, i.e., the difference in survival between responders and non-responders. Related to Fig. 5.

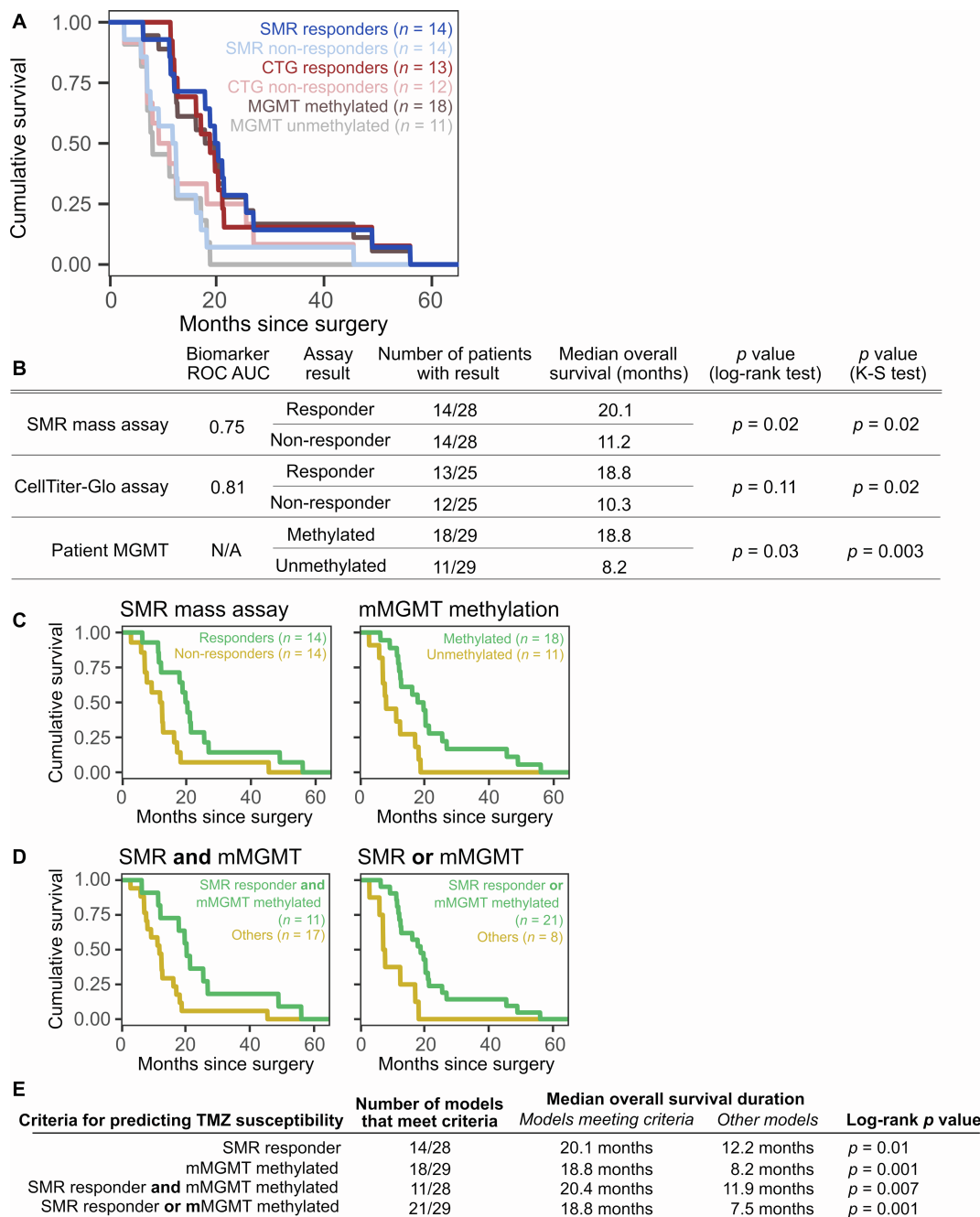


**Figure S5. Assessing the predictive power of functional and genomic biomarkers. (A)** Evaluating the ability of the SMR, CTG, and MGMT biomarkers to predict overall survival duration. Survival distributions for patients classified as TMZ responders versus non-responders by the SMR mass assay, the CTG assay, or MGMT promoter methylation. **(B)** Detailed statistics for evaluating the ability of each biomarker to predict overall survival duration. Related to Fig. 5. **(C)** Combining functional and genomic biomarkers to predict patient outcome. We defined new predictors of TMZ sensitivity based on combinations of the SMR and MGMT biomarkers. Specifically, we computed the survival distributions of patients who were (1) SMR responders *and* mMGMT-methylated, and (2) SMR responders *or* mMGMT-methylated. Fig. S5C shows survival distributions for patients stratified by single biomarkers. **(D)** Survival distributions for patients stratified by the combination of the SMR functional biomarker and the mMGMT methylation biomarker. **(E)** Summary statistics comparing the predictive power of combining functional biomarkers with MGMT to predict TMZ susceptibility. Depending on the criteria used to classify patients as likely TMZ-sensitive, one can achieve the desired level of sensitivity and specificity for predicting survival duration. Related to Fig. 5.